

A model of the sound generated by breaking waves

M. R. Loewen and W. K. Melville

R. M. Parsons Laboratory, Massachusetts Institute of Technology, Cambridge, Massachusetts 02139

(Received 15 November 1990; revised 3 March 1991; accepted 3 May 1991)

The sound produced from a single bubble, oscillating at its breathing mode frequency, and the bubble size distribution are used to model the sound produced by breaking waves. The data of Medwin and Daniel [J. Acoust. Soc. Am. **88**, 408–412 (1990)] is used to evaluate the performance of the model. The model generates a damped sinusoidal pulse for every bubble formed, as calculated from the bubble size distribution. If the range from the receiver to the breaker is known then the only unknown parameters are ϵ , the initial fractional amplitude of the bubble oscillation, and L , the dipole moment arm. It is found that if the product $\epsilon \times L$ is independent of the bubble radius the model reproduces the shape and magnitude of their measured sound spectrum accurately. The success of this simple model implies that the inverse problem (calculation of the bubble size distribution from the sound power spectrum) may be solved without the need to explicitly identify individual bubble pulses in the acoustic time series.

PACS numbers: 43.30.Nb

INTRODUCTION

Ambient sound levels in the ocean were first observed to correlate with wind speed by Knudsen *et al.*¹ in 1948. They found that spectral levels of “ambient noise from water motion” decreased with increasing frequency at a rate of 5 to 6 dB per octave in the frequency range 100 Hz to 25 kHz. They postulated that the water noise was primarily caused by breaking waves at the sea surface. In 1962, Wenz² reviewed the available oceanic ambient noise data and found the same – 5- to – 6-dB spectral slope. He concluded that the observed shapes and amplitudes of the spectra supported the hypothesis that gas bubbles, cavitation and spray at the surface were the source of the sound in the range 100 Hz to 20 kHz.

Kerman,³ Farmer and Vagle,⁴ and Pumphrey and Ffowcs Williams⁵ have attributed the wind dependence of oceanic sound to the increasing frequency and density of breaking waves as the wind speed increases. It has recently been shown by Melville *et al.*⁶ and Loewen and Melville⁷ that the acoustic energy radiated by breaking waves in the laboratory correlates with the mechanical wave energy dissipated and with the wave slope prior to breaking. However, there is still speculation as to which physical mechanisms are responsible for the sound produced by breaking waves.

Mechanisms suggested in the literature include bubbles bursting at the free surface,⁸ collective bubble cloud oscillations,⁹ splitting and coalescence of bubbles,⁸ and linear and nonlinear bubble oscillations.^{8–12} Banner and Cato⁸ observed that bubbles bursting at the free surface did not produce significant sound. Prosperetti and Lu¹³ showed that bursting bubbles radiate most of the sound energy into the air and only a small amount into the water. Bubbles splitting and coalescing were observed by Banner and Cato⁸ to correlate with some of the “dominant noise bursts.”

Collective bubble cloud oscillations may be an important source of sound at frequencies below 1 kHz (Ref. 14), but experimental confirmation of their importance as a

source of sound in the ocean remains elusive. A recent paper by Yoon *et al.*¹⁴ presents the first experimental evidence that bubbles within cylindrically shaped clouds oscillate collectively. However, the authors themselves question the relevance of the chosen geometry to oceanic conditions.

There appears to be a growing consensus that the primary source of sound from breaking waves is the oscillation of newly formed bubbles.^{5,8,10,15–17} Experimental evidence suggests that the newly created bubbles oscillate at their linear resonant frequency.^{5,8,15–17} Banner and Cato⁸ used a “quasisteady” breaking wave generated by a submerged air-foil to model a breaking wave in the laboratory. Using high-speed movies and hydrophone measurements, they found that “noise bursts” observed beneath the breaker were correlated with the formation of bubbles at the leading edge of the breaker and with coalescence and splitting of bubbles. Unfortunately, they did not present sound spectra and bubble size data sampled simultaneously for the same breaking wave.

Pumphrey and Crum¹⁵ studied the impact of water drops on a free surface using high-speed movies and sound measurements. They found that when the impacting drop entrains an air bubble, the majority of the sound produced is due to volume pulsations of the bubble. This mechanism is quite different from a breaking wave; however, there may be considerable splashing and spray associated with violent breaking waves.

Recently, Pumphrey and Ffowcs Williams⁵ used a steady flow over a weir in a laboratory flume to model breaking. They observed that newly created bubbles began radiating sound the instant they were formed. By comparing the frequency of oscillation with the predicted linear values they deduced that the sound was produced by volume pulsations of the bubbles.

Updegraff¹⁶ studied the sound radiated by gently spilling breaking waves in the ocean using hydrophone measurements and video recordings. He found that the acoustic spectrum from a small spilling wave had a slope of – 5 dB per

octave and that the sound was composed of damped sinusoidal pulses. He also observed that the peak oscillation pressures (referenced to 1 m and based on spherical spreading losses) for 81 pulses recorded during 14 small breaking waves were scattered between 0.2 and 1.2 Pa and had no significant dependence on frequency.

Some of the strongest experimental evidence to date in support of the hypothesis that newly created bubbles oscillating at their linear resonant frequency are the dominant source of sound beneath breaking waves has been provided by Medwin and his co-workers.^{17,18} Utilizing an anechoic wave tank, they have shown that the sound produced under gently spilling laboratory breaking waves is composed of a number of damped sinusoidal pulses. The damping rates of these pulses were found to be consistent with theoretical predicted values. Combined with previous results,^{5,8,15,16} this is convincing evidence that the source of the sound is newly created bubbles oscillating at their linear resonant frequency. Medwin and Daniel¹⁸ did not report the dipole strength as a function of bubble size and therefore it is not possible to directly confirm that their measured sound spectrum is consistent with their measured bubble population.

Bubbles that are formed at the free surface are not in equilibrium initially and must relax to an equilibrium spherical shape. It is this relaxation process that leads to the linear oscillation of the bubbles at the lowest mode (i.e., breathing mode) which has a frequency given by¹⁹

$$\omega_b = (1/a)(3\gamma P_0/\rho)^{1/2}, \quad (1)$$

where ω_b is the resonant radian frequency of the breathing mode, a is the equilibrium radius of the bubble, γ is the ratio of the specific heats of the bubble gas, P_0 is the ambient bubble pressure, and ρ is the density of water. Longuet-Higgins^{11,12} has presented a nonlinear theory which proposes that the asymmetric or "shape" oscillations of the newly created bubbles produce significant sound energy. The search for experimental evidence that this mechanism is important remains an area of active research but to date the results are inconclusive.

Medwin and Daniel¹⁸ used Eq. (1) to calculate the bub-

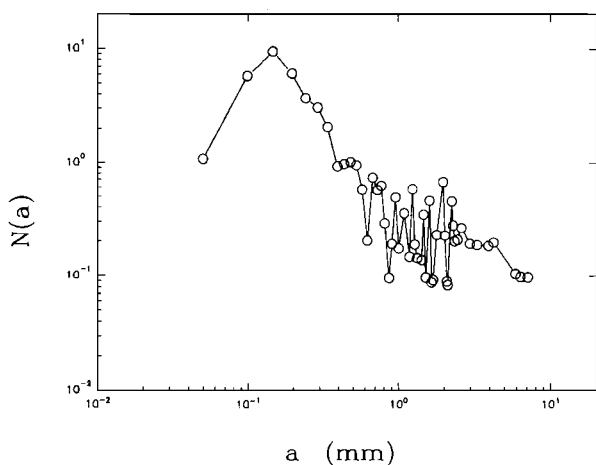


FIG. 1. $N(a)$ the number of bubbles per wave in the radius interval from $(a_i + a_{i-1})/2$ to $(a_{i+1} + a_i)/2$ centered at a_i , from Medwin and Daniel.¹⁸

ble size distribution from the sound data. [Since Medwin and Daniel used an acoustic method to measure the bubble size distribution, it may seem that the work described here is tautological. This is not the case. According to this model, the relationship between the bubble size distribution and the sound spectrum produced depends on the dipole strength as a function of bubble size. It is our simple hypothesis regarding the dipole strength (or equivalently $\epsilon \times L$) that supplements the measurements and leads to the success of the model.] In Fig. 1, we have plotted their bubble size distribution data recomputed to show the number of bubbles per wave per radius increment. A plot of their measured sound spectrum is shown in Fig. 2. The sound spectrum and bubble size data were obtained from two separate series of experiments. The sound spectrum was averaged over six breaking waves and the bubble size distribution data was measured from a series of ten breakers.²⁰ By using a simple dipole model of the sound generated by individual bubbles, we will demonstrate that the measured sound spectrum may be simply related to the measured bubble size distribution. It will also be shown that Medwin and Daniel's data and our model both support the hypothesis that low-frequency sound may be generated under breaking waves without recourse to collective bubble cloud oscillations: Observed single bubbles oscillating at their lowest mode may radiate sound at frequencies below 500 Hz.

I. FORMULATION

In Fig. 3, a sketch of the basic geometry and definitions of some of the parameters is shown. A bubble oscillating close to a free surface will radiate sound as a dipole. If $kL < 1$ and $ka \ll 1$, the pressure field produced by a single bubble radiating can be written as^{21,22}

$$p(t - t_i) = \left(\frac{3\gamma P_0}{\rho} \right)^{3/2} \frac{\rho \epsilon d L}{R^2 c} e^{-\omega_b \delta (t - t_i)/2} \times \left(\sin(\omega_b (t - t_i)) - \frac{\cos(\omega_b (t - t_i))}{kR} \right) \times H(t - t_i), \quad (2)$$

where k is the acoustic wave number, d is the receiver depth,

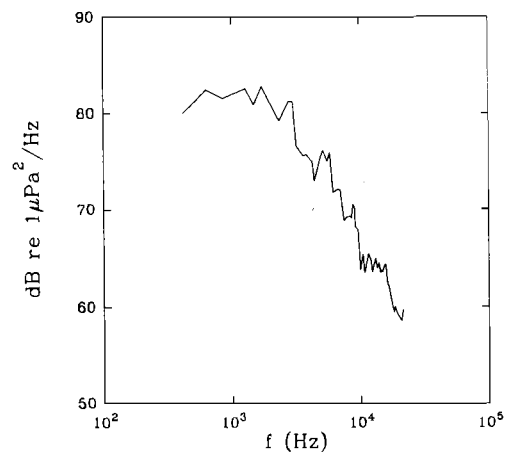


FIG. 2. Measured sound power spectrum, averaged over six gently spilling waves, data from Medwin and Daniel.¹⁸

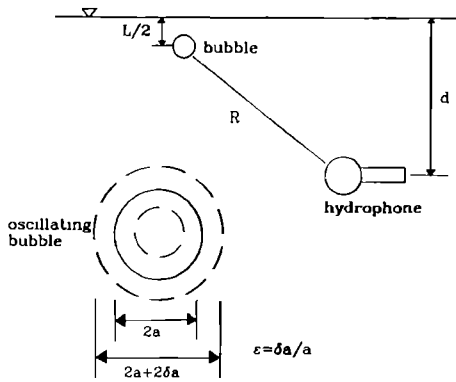


FIG. 3. Sketch of the geometry of the problem and definitions of some of the parameters.

R is the range from the receiver to the bubble, c is the speed of sound in water, L is twice the distance from the bubble center to the free surface, δ is the damping constant, t_i is the time at which the oscillations begin, ϵ is the amplitude of the bubble surface oscillations divided by the equilibrium bubble radius, and $H(t)$ is the Heaviside unit step function. For bubbles from 50- μm to 7-mm radius oscillating near a free surface, it has been shown that radiation and viscous damping are negligible compared to thermal damping.^{10,23} Crowther¹⁰ has shown that Devin's²³ equation [Devin's Eq. (68)] for the thermal damping constant could be approximated to within a few percent for frequencies below 60 kHz by

$$\delta(f) = (4.4 \times 10^{-4} f^{0.5}) / (1 + f/2.5 \times 10^5), \quad (3)$$

where f is the resonant bubble oscillation frequency in Hz. [In this and subsequent equations dependent on δ , SI units are applicable.]

The power spectrum of an individual bubble pulse as given by Eq. (2) is

$$g(\omega; \omega_b) = (3\gamma P_0 / \rho)^3 (\rho \epsilon dL / R^2 c)^2 \times \{ [\omega_b^2 (\delta - 2kR)^2 + 4\omega^2] / [(kR)^2 (\delta \omega_b)^2 + 4(\omega_b - \omega)^2 (\delta \omega_b)^2 + 4(\omega_b + \omega)^2] \}. \quad (4)$$

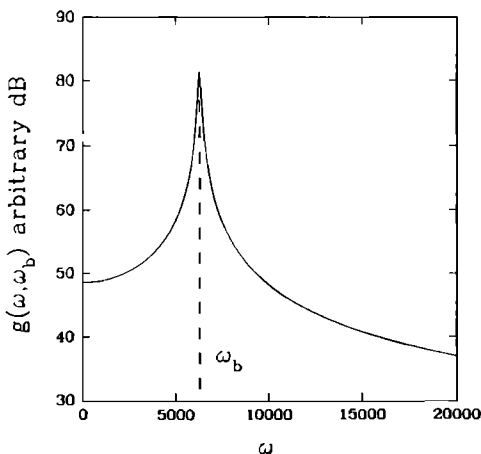


FIG. 4. The power spectrum of an individual bubble pulse $g(\omega; \omega_b)$ as given by Eq. (4).

Figure 4 shows a plot of Eq. (4) and it is evident that the energy is concentrated in a very small band around ω_b .

The sound spectrum is modeled by reproducing the bubble size distribution of Medwin and Daniel's¹⁸ for a given number of bubbles, K . The total sound spectrum is the sum of the individual bubble pulse spectra calculated from Eq. (4). The inputs to the model are: (1) K the total number of bubbles; (2) Medwin and Daniel's bubble size distribution; (3) ϵ , L , R_{\min} , and R_{\max} . In Fig. 1 is a plot of the measured bubble size distribution $N(a)$ (Ref. 18). It is a set of discrete points N_i which specify the number of bubbles that are created by one gently spilling wave in the radius interval from $(a_i + a_{i-1})/2$ to $(a_i + a_{i+1})/2$ centered at the radius a_i . The number of bubbles, n_i , in the radius interval centered at a_i is given by

$$n_i = \frac{K}{\sum_{i=1}^m N_i} N_i. \quad (5)$$

The model randomly distributes the n_i bubbles across the radius interval centered at a_i . The range R was varied randomly between R_{\min} and R_{\max} and ϵ and L where kept constant for a given run. The final sound power spectrum is given by

$$G(\omega) = \sum_{i=1}^K g(\omega; \omega_i), \quad (6)$$

where ω_i corresponds to a_i through Eq. (1).

In order to check the results obtained by this method, (which we called the analytic spectrum model) a second Monte Carlo method was used. It simulates the sound pressure time series directly. It evaluates Eq. (2) for each bubble formed and produces a time series from the sum of the individual bubble pulse time series. Inputs to the model are: (1) K the number of bubbles; (2) Medwin and Daniel's bubble size distribution; (3) R_{\min} , R_{\max} , ϵ_{\min} , ϵ_{\max} , L_{\min} , L_{\max} and t_{\max} . The number of bubbles in each radius interval is calculated as outlined for the analytic spectrum model. The model starts each bubble pulse at a random time between $t = 0$ and $t = t_{\max}$. For each bubble, R , ϵ , and L are varied randomly between the corresponding minimum and maximum values. The sound pressure time series of the ensemble of oscillating bubbles is given by

$$P(t) = \sum_{i=1}^K p_i(t - t_i), \quad (7)$$

where $p(t - t_i)$ is given by Eq. (2). The sound spectrum is then calculated using standard signal processing techniques.

Spectra computed by the two methods are shown compared in Fig. 5. They are seen to produce very similar results when the mean values of ϵ and L in the Monte Carlo model are set equal to the constant values of ϵ and L used in the analytic spectrum model. This suggests that the sound spectrum is insensitive to the higher-order statistical moments of the parameters.

Both models contain a certain amount of randomness. They both distribute the bubbles randomly across a given bubble radius interval, they both randomly vary the range between a minimum and maximum value and the second Monte Carlo method varies ϵ and L randomly between minimum and maximum values. In Fig. 6, we have plotted a

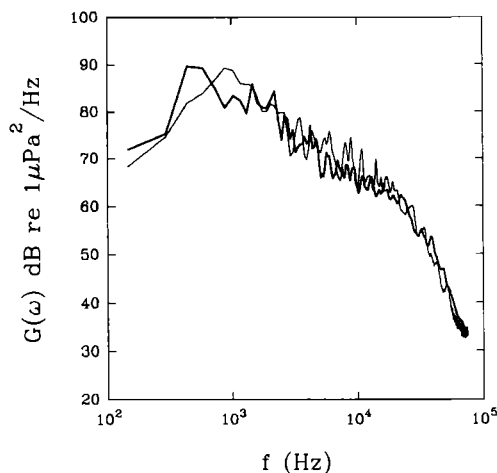


FIG. 5. A comparison of the sound spectrum calculated using the analytic spectrum model, plotted with the bold line, and the Monte Carlo model, plotted with the thin line.

mean spectrum averaged from ten spectra modeled with the analytic spectrum model and the 95% confidence limits. This figure indicates that the randomness of the model results in ± 3 to ± 4 dB of variation in the amplitude of the modeled spectrum. As a result we would not expect modeled spectra to match measured spectra closer than these limits.

II. RESULTS

The goal of this study was to show that the bubble size distribution beneath a breaking wave could be used to calculate the sound-pressure spectrum. The values chosen for K , ϵ , L , and R will obviously determine how well the sound spectrum is predicted. Medwin and Daniel¹⁸ observed approximately 50 bubbles per wave and their sound-pressure spectrum (Fig. 2) was averaged over six waves therefore, $K = 300$, for all of the model runs. The depth of the hydrophone, d , in their experiments was 0.24 m. The range from

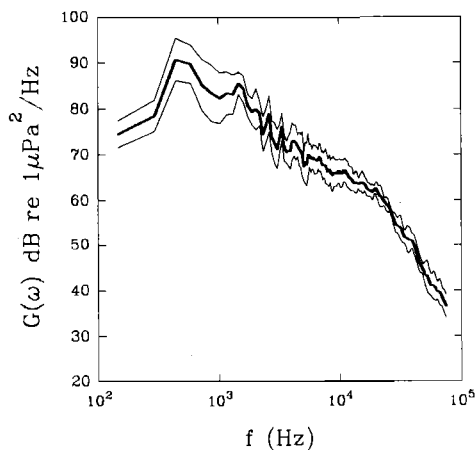


FIG. 6. The bold line is the mean spectrum averaged from ten spectra generated by the analytic spectrum model. The upper and lower lines are the 95% confidence limits.

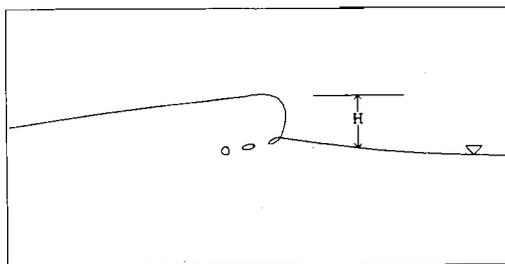


FIG. 7. Sketch of the formation of bubbles at the toe of the spilling region in a gently spilling wave.

the hydrophone to the bubbles was estimated from Figs. 12 and 13 of Daniel's²⁰ thesis which show the horizontal distribution of the bubbles in two breaking waves. These plots show that R varied from 0.24 m to approximately 0.5 m. Therefore, we set $R_{\min} = 0.24$ m and $R_{\max} = 0.5$ m for the model runs.

The values for ϵ and L were more difficult to estimate. Medwin and Beaky¹⁷ estimated the value of ϵ for a single bubble and found $\epsilon = 0.014$ for $a = 0.3$ mm. We assume that the value for L is of the order of the wave amplitude. This follows from the conjecture that in these gently spilling waves the bubbles are entrained at the toe of the spilling region as shown in Fig. 7. Medwin and Daniel¹⁸ do not provide any wave height data, but Daniel²⁰ states in his thesis that the maximum wave amplitude was 0.03 m. Therefore, we assume that $L = O(10^{-2}$ m) for the model runs.

In Fig. 8, the sound spectra produced by the Monte Carlo model with $\epsilon = 0.005$ – 0.025 and $L = 0.01$ – 0.03 m and Medwin and Daniel's spectrum are plotted. The modeled spectrum matches the amplitude and slope of the measured spectrum closely when ϵ and L are set to these physically realistic values. The bars indicate the 95% confidence limits of the modeled spectrum.

Results from the analytic spectrum model with

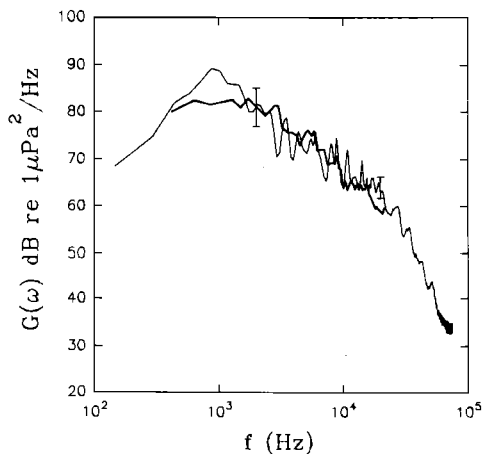


FIG. 8. Comparison of a sound spectrum from the Monte Carlo model with $\epsilon = 0.005$ – 0.025 and $L = 0.01$ – 0.03 m and the measured sound spectrum of Medwin and Daniel,¹⁸ plotted with a bold line. The bars indicate the 95% confidence limits of the modeled spectrum.

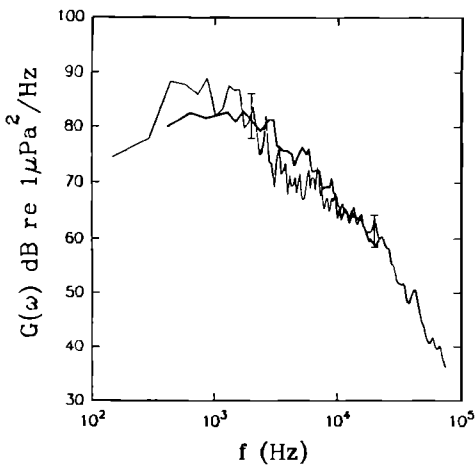


FIG. 9. Comparison of a sound spectrum from the analytic spectrum model with $\epsilon = 0.015$ and $L = 0.02$ m and the measured sound spectrum of Medwin and Daniel,¹⁸ plotted with a bold line. The bars indicate the 95% confidence limits of the modeled spectrum.

$\epsilon = 0.015$ and $L = 0.02$ m are shown in Fig. 9, compared to Medwin and Daniel's¹⁸ spectrum. The amplitude and slope of the modeled spectrum agree well with the observed data when ϵ and L are set equal to these values. The bars again indicate the 95% confidence limits of the modeled spectrum. These values of ϵ and L would give a maximum far-field dipole pressure 1 m on axis of 1.7 Pa.

III. DISCUSSION

We have shown that a simple model of the sound produced by a single oscillating bubble can be used to obtain the sound spectrum from the bubble size distribution under breaking waves. If the range R from the receiver to the breaker is known, then the model has only two unknown parameters ϵ and L . Our results indicate that the product $\epsilon \times L$ is not a function of the bubble radius a , but is effectively constant across the sound spectrum. This is supported by Updegraff's¹⁶ measurements which showed that the peak oscillation pressures were not a function of frequency.

It is possible that ϵ and L are functions of the wave geometry or the energy dissipation. For waves of moderate slope, Loewen and Melville⁷ found that the acoustic energy radiated by a breaking wave was approximately proportional to the energy dissipated and the wave slope. Longer or steeper waves might be expected to entrain bubbles to larger depths increasing the dipole moment L . Under larger breaking waves, L may increase because extremely large pockets of air are injected to greater depths initially, and when they break up to form smaller bubbles the dipole moment arm is of the order of the depth to which the pocket of air was initially injected. It could be the depth to which the large pockets of air are injected that scales with the wave parameters. It may also be that larger waves produce more sound simply because more air is entrained and, hence, more bubbles are formed.

The largest bubble that Medwin and Daniel¹⁸ observed had a radius of 7.4 mm, which corresponds to a resonant frequency of 440 Hz. We expect that bubbles considerably

larger than this will be present under waves larger than the 1.4-Hz and 0.03-m amplitude waves generated by Medwin and Daniel. Therefore, it should be possible for these larger bubbles to radiate sound at frequencies as low as several hundred Hz.

We believe that these results clearly demonstrate that bubble population data can be used to accurately and simply model the shape and the amplitude of the sound spectrum produced by a breaking wave. The more practical application would be to solve the inverse problem. That is, to calculate the bubble size distribution from the sound spectrum. If ϵ and L , or at least the product $\epsilon \times L$, is a constant as assumed in our model, then the problem is easily inverted.

If we assume that the energy in the sound spectrum at a given radian frequency ω_b is due only to bubbles corresponding to a radius a calculated from Eq. (1), the problem becomes even simpler. We are assuming that the spectrum of a single bubble pulse is a delta function which is a reasonable approximation, (see Fig. 4). The mean-square signal level for an individual bubble sound pulse is found by integrating Eq. (2) in time to give

$$\begin{aligned} \overline{p^2}(\omega_b) = & \left(\frac{3\gamma P_0}{\rho} \right)^3 \left(\frac{\rho \epsilon dL}{R^2 c} \right)^2 \left[\left(\frac{2}{\delta \omega_b (\delta^2 + 4)} \right) \right. \\ & + \left(\frac{\delta^2 + 2}{(kR)^2 (\delta \omega_b (\delta^2 + 4))} \right) \\ & \left. - \left(\frac{2}{kR \omega_b (\delta^2 + 4)} \right) \right], \end{aligned} \quad (8)$$

where $\overline{p^2}(\omega_b)$ is the mean square signal level of a bubble resonating at radian frequency ω_b . The mean square value of the signal within the frequency range $\omega_b - \Delta\omega$ and $\omega_b + \Delta\omega$ is given by²⁴

$$\varphi^2(\omega_b; \Delta\omega) = \int_{\omega_b - \Delta\omega/2}^{\omega_b + \Delta\omega/2} P(\omega) d\omega. \quad (9)$$

For the inverse problem, the input is the sound spectrum $P(\omega)$ which has a resolution of $\Delta\omega$. The number of bubbles in each frequency bin from $\omega_b - \Delta\omega$ to $\omega_b + \Delta\omega$ is then given by

$$n_i = \varphi^2(\omega_b; \omega_b) / \overline{p^2}(\omega_b), \quad (10)$$

if we assume the range R is the same for bubbles of a given radius. The complete bubble size distribution can be calculated by evaluating Eq. (10) in each frequency bin across the entire sound spectrum.

ACKNOWLEDGMENTS

This work was supported by a grant from the Office of Naval Research (Ocean Acoustics). We thank H. Medwin for making available detailed descriptions of his published data.

¹V. O. Knudsen, R. S. Alford, and J. W. Emling, "Underwater ambient noise," *J. Mar. Res.* **7**, 410-429 (1948).

²G. M. Wenz, "Acoustic ambient noise in the ocean: Spectra and sources," *J. Acoust. Soc. Am.* **34**, 1936-1956 (1962).

³B. R. Kerman, "Underwater sound generation by breaking wind waves,"

- J. Acoust. Soc. Am. **75**, 149–165 (1984).
- ⁴D. Farmer and S. Vagle, "On the determination of breaking wave distributions using ambient sound," J. Geophys. Res. **93**, 3591–3600 (1988).
- ⁵H. C. Pumphrey and J. E. Ffowcs Williams, "Bubbles as sources of ambient noise," IEEE J. Oceanic Eng. **15**, 268–274 (1990).
- ⁶W. K. Melville, M. R. Loewen, F. C. Felizardo, A. T. Jessup, and M. J. Buckingham, "Acoustic and microwave signatures of breaking waves," Nature **336**, 54–59 (1988).
- ⁷M. R. Loewen and W. K. Melville, "Microwave backscatter and acoustic radiation from breaking waves," J. Fluid Mech. **224**, 601–623 (1991).
- ⁸M. L. Banner and D. H. Cato, "Physical mechanisms of noise generation by breaking waves," in *Sea Surface Sound*, edited by B. R. Kerman (Kluwer Academic, Boston, 1988), pp. 429–436.
- ⁹A. Prosperetti, "Bubble dynamics in oceanic ambient noise," in *Sea Surface Sound*, edited by B. R. Kerman (Kluwer Academic, Boston, 1988), pp. 151–171.
- ¹⁰P. A. Crowther, "Bubble noise creation mechanisms," in *Sea Surface Sound*, edited by B. R. Kerman (Kluwer Academic, Boston, 1988), pp. 131–150.
- ¹¹M. S. Longuet-Higgins, "Monopole emission of sound by asymmetric bubble oscillations. Pt. 1: Normal modes," J. Fluid Mech. **201**, 525–542 (1989).
- ¹²M. S. Longuet-Higgins, "Monopole emission of sound by asymmetric bubble oscillations. Pt. 2: An initial value problem," J. Fluid Mech. **201**, 543–565 (1989).
- ¹³A. Prosperetti and N. Q. Lu, "Cavitation and bubble bursting as sources of oceanic ambient noise," J. Acoust. Soc. Am. **84**, 1037–1097 (1988).
- ¹⁴S. W. Yoon, L. A. Crum, A. Prosperetti, and N. Q. Lu, "An investigation of the collective oscillations of a bubble cloud," J. Acoust. Soc. Am. **89**, 700–706 (1991).
- ¹⁵H. C. Pumphrey and L. A. Crum, "Acoustic emissions associated with drop impacts," in *Sea Surface Sound*, edited by B. R. Kerman (Kluwer Academic, Boston, 1988), pp. 463–483.
- ¹⁶G. E. Updegraff, "In situ investigation of sea surface noise from a depth of one meter," Ph. D. Thesis, University of California, San Diego (1989).
- ¹⁷H. Medwin and M. M. Beaky, "Bubble sources of the Knudsen sea noise spectra," J. Acoust. Soc. Am. **86**, 1124–1130 (1989).
- ¹⁸H. Medwin and A. C. Daniel Jr., "Acoustical measurements of bubble production by spilling breakers," J. Acoust. Soc. Am. **88**, 408–412 (1990).
- ¹⁹M. Minnaert, "On musical air bubbles and the sound of running water," Philos. Mag. **16**, 235–248 (1933).
- ²⁰A. C. Daniel Jr., "Bubble production by breaking waves," Master's Thesis, Naval Postgraduate School, Monterey, CA (1989).
- ²¹C. S. Clay and H. Medwin, *Acoustical Oceanography* (Wiley, New York, 1977), pp. 452–453.
- ²²P. M. Morse and K. U. Ingard, *Theoretical Acoustics* (McGraw-Hill, New York, 1968), p. 312.
- ²³C. Devin, "Survey of thermal, radiation, and viscous damping of pulsating air bubbles in water," J. Acoust. Soc. Am. **31**, 1654–1667 (1959).
- ²⁴J. S. Bendat and A. G. Piersol, *Random Data, Analysis and Measurement Procedures* (Wiley-Interscience, New York, 1986), 2nd ed., pp. 134–135.